REFERENCES AND NOTES

1. J. S. Miller *et al.*, *Chem. Commun.* **1986,** 1026 (1986).
2. J. S. Miller *et al.*, *J. Am. Chem. Soc.*, in press.
3. J. S. Miller, A. J. Epstein, W. M. Reiff, *Isr. J. Chem.*, in press.
4. G. A. Candela, L. Swarzendruber, J. S. Miller, M. J. Rice, *J. Am. Chem. Soc.* **101,** 2755 (1979).
5. $C_4(CN)_6$ = percyano-1,3-butadiene; $C_6(CN)_6$ = hexacyanotrimethylenecyclopropane; TCNQ = 7,7,8,8-tetracyano-*p*-quinodimethane; $TCNQF_4$ = perfluoro-TCNQ; DDQ = 2,3-dichloro-5,6-dicyanobenzoquinone; TCNE = tetracyanoethylene; $TCNQ(CN)_4$ = percyano-TCNQ.
6. J. H. Zhang, W. M. Reiff, J. S. Miller, unpublished results.
7. The following crystallographic analysis was performed by Oneida Research Services; space group = $P2_1/c$; a = 9.382 (± 0.004) Å; b = 11.797 (± 0.002) Å; c = 19.520 (±0.009) Å; β = 98.34°; V = 2138 (± 2) Å^3; Z = 2, R_w = 8.1%, where a, b, and c are the lengths and β is the angle that define the unit cell, V is the volume of the unit cell, Z is the number of molecules in the unit cell, and R_w is the weighted agreement factor. Full crystallographic data will be deposited in the Cambridge Crystallographic Database.
8. D. A. Dixon, J. C. Calabrese, J. S. Miller, *J. Am. Chem. Soc.* **108,** 2582 (1986).
9. J. S. Miller *et al.*, *ibid.*, p. 449.
10. J. S. Miller *et al.*, unpublished results.
11. D. P. Freyberg, J. L. Robbins, K. N. Raymond, J. C. Smart, *J. Am. Chem. Soc.* **92,** 892 (1971).
12. The STO-3G basis set has 1*s*, 2*s*, and three 2*p* functions on carbon, nitrogen, and oxygen. For chlorine, there are 1*s*, 2*s*, 3*s*, three 2*p*, and three 3*p* functions. These are formed by contracting three Gaussian functions for each basis function as described by W. J. Hehre, R. F. Stewart, and J. A. Pople [*J. Chem. Phys.* **51,** 2657 (1969)].
13. HONDO is a general ab initio molecular orbital program system as described by M. Dupuis, J. Rys, and H. F. King, [*ibid.* **65,** 111 (1965)] and H. F. King, M. Dupuis, and J. Rys [*National Resource for Computer Chemistry Software Catalog* (National Resource for Computer Chemistry, Berkeley, CA, 1980), vol. 1, program QHO2 (HONDO) (available from University of California, Berkeley)].
14. GRADSCF is an ab initio gradient program system designed and written by A. Komornicki at Polyatomics Research, Mountain View, CA, and supported by grants through the NASA-Ames Research Center.
15. A. Komornicki, K. Ishida, K. Morokuma, R. Ditchfield, M. Conrad, *Chem. Phys. Lett.* **45,** 595 (1977).
16. P. Pulay, in *Applications of Electronic Structure Theory,* H. F. Schaefer III, Ed. (Plenum, New York, 1977), chap. 4.
17. H. F. King and A. Komornicki, *J. Chem. Phys.* **84,** 5645 (1986).
18. L. E. Sutton, *Tables of Interatomic Distances and Configuration in Molecule and Ions, Supplement, Special Publication No. 18* (Chemical Society, London, 1965), p. 20s.
19. The C–Cl bond lengthens by 0.05 Å in $(DDQ)^{2-}$ as compared to DDQ.
20. The STO-3G basis set has 78 basis functions and the DZD basis set has 148 basis functions. The calculations scale as N^4, where N is the number of basis functions.
21. The *s* and *p* basis set for carbon, nitrogen, and oxygen is from T. H. Dunning, Jr., and P. J. Hay [in *Methods of Electronic Structure Theory,* H. F. Schaefer III, Ed. (Plenum, New York, 1977), chap. 1]. The *s* and *p* basis set for chlorine is from A. D. McLean and G. S. Chandler [*J. Chem. Phys.* **72,** 5639 (1980)].
22. J. Breulet *et al.*, *J. Am. Chem. Soc.* **106,** 6250 (1984).
23. D. A. Dixon and J. S. Miller, unpublished results.
24. The scale factor 0.82 is taken from the ratio of ν_{expt} to ν_{calc} given in (*10*).

29 September 1986; accepted 30 December 1986

Conservation of Brain Amyloid Proteins in Aged Mammals and Humans with Alzheimer's Disease

DENNIS J. SELKOE, DOUGLAS S. BELL, MARCIA B. PODLISNY, DONALD L. PRICE, LINDA C. CORK

The formation of clusters of altered axons and dendrites surrounding extracellular deposits of amyloid filaments (neuritic plaques) is a major feature of the human brain in both aging and Alzheimer's disease. A panel of antibodies against amyloid filaments and their constituent proteins from humans with Alzheimer's disease cross-reacted with neuritic plaque and cerebrovascular amyloid deposits in five other species of aged mammals, including monkey, orangutan, polar bear, and dog. Antibodies to a 28–amino acid peptide representing the partial protein sequence of the human amyloid filaments recognized the cortical and microvascular amyloid of all of the aged mammals examined. Plaque amyloid, plaque neurites, and neuronal cell bodies in the aged animals showed no reaction with antibodies to human paired helical filaments. Thus, with age, the amyloid proteins associated with progressive cortical degeneration in Alzheimer's disease are also deposited in the brains of other mammals. Aged primates can provide biochemically relevant models for principal features of Alzheimer's disease: cerebrovascular amyloidosis and neuritic plaque formation.

ALZHEIMER'S DISEASE (AD) IS AN age-related brain degenerative disease that is the most common cause of intellectual failure in late life. The cerebral cortex of patients with AD contains intraneuronal masses of cytoplasmic filaments [neurofibrillary tangles (NFTs)] and clusters of degenerating axons and dendrites (neuritic or senile plaques) (*1*). In many cases, these degenerating neurites surround a core of extracellular proteinaceous filaments that have the structural and tinctorial properties of amyloid. In most cases of AD, morphologically and immunochemically identical amyloid filaments also occur in the walls of some capillaries, arterioles, and small arteries in the cerebral cortex and in some meningeal arteries (*2–5*). In an electron microscopic study, every neuritic plaque examined by serial sectioning in six cases of AD contained a capillary with amyloid filaments at its basement membrane (*6*). Neuritic plaques and NFTs occur in abundance in AD; however, a smaller number of qualitatively identical lesions occur in restricted topographic distribution in the brains of most neurologically normal aged humans (*7*).

The lack of a naturally occurring analog of AD in animals has been a major obstacle to studying the pathogenesis of the disease. An animal model that shows cortical neuritic degeneration and deposition of amyloid fibers that are biochemically closely related to or the same as those in aged humans could facilitate understanding of the genesis of neuritic plaques and microvascular amyloidosis. Aged monkeys and dogs develop plaques in the cerebral cortex (*8–11*) that are composed of neurites from multiple neurotransmitter systems (*10–12*) surrounding deposits of amyloid (*8, 9*). We have now shown that the amyloid in senile plaques and cerebral vessels in three species of aged nonhuman primates, in dogs, and in a polar bear cross-react with a panel of antibodies raised against human senile plaque amyloid and its constituent proteins.

We examined the brains of three rhesus monkeys (*Macaca mulatta*) (30, 31, and 31 years of age; equivalent human age ~90 years); an orangutan (*Pongo pygmaeus*) that died naturally in a zoo (46 years); two squirrel monkeys (*Saimiri sciureus*) (20 and 23 years); nine dogs (12 to 16 years) that died of natural causes; and a polar bear (*Ursus maritimus*) (28 years) that was killed by euthanasia in a zoo. Brains were fixed by immersion in 10% buffered Formalin except for one monkey, which was anesthetized and perfused with 4% paraformaldehyde. Blocks of neocortex were embedded in paraffin, and 10- to 15-μm coronal sections were cut and mounted on albuminized slides for immunocytochemistry. We used several rabbit antisera (Table 1). Two of these, designated S and V, were raised against partially purified fractions of human paired helical filaments (PHFs) prepared from cerebral cortex of patients with AD (*13*). Because such PHF-enriched fractions contain variable amounts of contaminating am-

D. J. Selkoe, D. S. Bell, M. B. Podlisny, Department of Neurology (Neuroscience), Harvard Medical School, and Center for Neurologic Diseases, Department of Medicine (Neurology), Brigham and Women's Hospital, Boston, MA 02115.
D. L. Price and L. C. Cork, Division of Comparative Medicine and Neuropathology Laboratory, Departments of Pathology, Neurology and Neuroscience, Johns Hopkins University School of Medicine, Baltimore, MD 21205.

Table 1. Reactivities of antisera to human amyloid to amyloid deposits from the brains of humans and animals. Key: 0, no reaction; 1, light brown immunoperoxidase reaction; 2, medium brown; 3, medium-dark brown; 4, dark brown; BV, cortical and meningeal blood vessel amyloid deposits.

Anti-serum	Immunogen (human)	Human		Rhesus monkey (n = 3)		Orangutan (n = 1)		Squirrel monkey (n = 2)		Dog (n = 9)		Polar bear (n = 1)	
		BV	Plaques	BV	Plaques	BV	Plaques	BV	Plaques	BV	Plaques	BV*	Plaques
A	4- to 7-kD amyloid protein	4	3–4	4	3–4	3–4	2	3–4	3–4	2	2–3		1
S	Amyloid filaments	4	3–4	4	3–4	2–3	1–2	3–4	3–4	1–2	1–3		1
C	4- to 7-kD amyloid protein	3	2	3–4	1–2	3–4	1–2	3	3	1–2	1–2		1
B	Synthetic amyloid peptide	4	1	3–4	2–3	1	0–1	2–3	2	1	1		1
V	Amyloid filaments	3	1–2	1–2	1	1	0	0–1	0–1	0	0		0
P	PHF	0	0	0	0	0	0	0	0	0	0		0

*Thioflavin staining revealed no amyloidotic blood vessels in the polar bear section.

yloid filaments (*5*) and because these two rabbits had each received injections of immunogen approximately 12 times over 3 years, the resultant mixed antisera labeled PHF-containing plaque neurites and NFTs as well as amyloid in plaque cores and cortical and meningeal vessels (in both AD and normal aged human brain). Absorption experiments with either purified senile plaque cores (*5*) or the microtubule-associated phosphoprotein tau (*14*) showed that S and V were mixed antisera containing two distinct populations of antibodies—those directed against amyloid filaments and those directed against PHFs [and against the altered tau proteins in PHF (*14, 15*)]. Two other antisera, designated A and C, were produced against a protein (~4 to 7 kD) that had been extracted with formic acid from AD amyloid filaments and purified by size-exclusion high-performance liquid chromatography (*5*); these antisera label senile plaque and vascular amyloid in AD and normal aged brain. A fifth rabbit (designated B) had been immunized with a synthetic 28–amino acid peptide with the NH_2-terminal sequence of an AD cerebrovascular amyloid protein (*3, 16*); the resulting antiserum also labels plaque cores and amyloidotic vessels in AD and aged brain. A sixth rabbit (designated P) had been immunized only twice with highly purified PHF fractions, resulting in a high-titer antiserum specific for PHFs (that is, for NFTs and plaque neurites), which showed no reaction with amyloid (*13*). We also used a polyclonal antibody (DJ) to heat-stable microtubule-associated proteins (tau and MAP2) from rat brain and a monoclonal antibody (RT97) to a phosphorylated epitope of the 200-kD neurofilament protein (*17*). Both DJ and RT97 label essentially all NFTs and plaque neurites in AD brain, but do not label amyloid deposits. A preimmune rabbit serum also served as a negative control. Sections of human cortex from patients with Alzheimer's disease (age range, 60 to 86 years) that contained abundant senile plaques and vascular amyloid were the positive controls.

Amyloid-bearing senile plaques could be identified by their characteristic fluorescence after reaction with thioflavin-S in the frontal, temporal, or parietal cortex of the three aged rhesus monkeys, the two squirrel monkeys, and the orangutan. Such plaques were labeled by silver staining (Bielschowsky method) and showed the green-red birefringence of amyloid deposits under polarized light after being stained with Congo red. In addition to amyloid plaques, certain intracortical and meningeal microvessels (ranging in diameter from 10 to 200 μm) also showed thioflavin-positive amyloid deposits in their walls. In all nine 12- to 16-year-old dogs, thioflavin-positive amyloid deposits were seen in some meningeal arteries and cortical capillaries. In temporo-parietal cortex, the number of amyloid-bearing meningeal vessels ranged from 2 to more than 20 per section, and in occipital lobe, from 3 to more than 40 per section. Two dogs displayed abundant (more than 20 per section) thioflavin-positive amyloid plaques in both hippocampal and occipital sections, whereas three dogs had only one to six plaques per section and four had none. Two control dogs aged 2 and 5 years, respectively, showed no amyloid deposits whatsoever. In the aged polar bear, small numbers (fewer than eight per section) of thioflavin-positive plaques were found at the depths of some cortical sulci; amyloid-bearing blood vessels were not seen.

All five antisera (A, S, C, B, and V) that are known to label vascular and plaque amyloid in human brain (for example, Fig. 1, A and C) also stained the amyloid plaques and amyloid-bearing cortical and meningeal vessels in all of the primate brains (Table 1; Fig. 1, B and E, and Fig. 2, A, B, and C). Reaction of representative sections with thioflavin before immunolabeling confirmed that the amyloid deposits were selectively immunostained (Fig. 1, D and E). In the dogs, the amyloid deposits found in small meningeal arteries were reactive with amyloid antisera A and S (Fig. 2D). The latter sera consistently produced the most intense amyloid staining in all species examined, including humans (Table 1). The senile plaques observed in the cortex of five of the dogs were strongly positive with these antisera (Fig. 2D, inset). In the polar bear, the occasional senile plaques found at the depths of some cortical sulci showed modest but definite reaction with four of the five amyloid antisera (Table 1 and Fig. 2E); no amyloid-bearing blood vessels were seen in these sections.

Antiserum P (PHF- and tau-specific) and preimmune rabbit serum produced no staining in the animal brains, although antiserum P strongly stained NFTs and senile plaque neurites in human brains (*13*). The polyclonal tau-MAP2 antibodies (DJ) and the neurofilament monoclonal (RT97) labeled neither the amyloid cores of senile plaques nor the vessels in any species. RT97, which stains the neurites of senile plaques in AD brain, produced a similar neuritic pattern in the plaques of aged rhesus monkeys, whereas neither tau-reactive antiserum (P or DJ) labeled plaque neurites.

We compared the relative intensities of animal and human amyloid reactivity with each of our five amyloid antisera at a standard dilution (1:250) (Table 1). Two observers independently scored the intensity of the peroxidase reaction on the amyloid in each species without knowledge of the antiserum used. In each animal, antisera A and S produced the strongest staining and identified the largest number of amyloid deposits, followed by C, B, and V; the patterns were similar in all six species.

Pre-absorption of antisera A and S with partially purified senile plaque amyloid cores

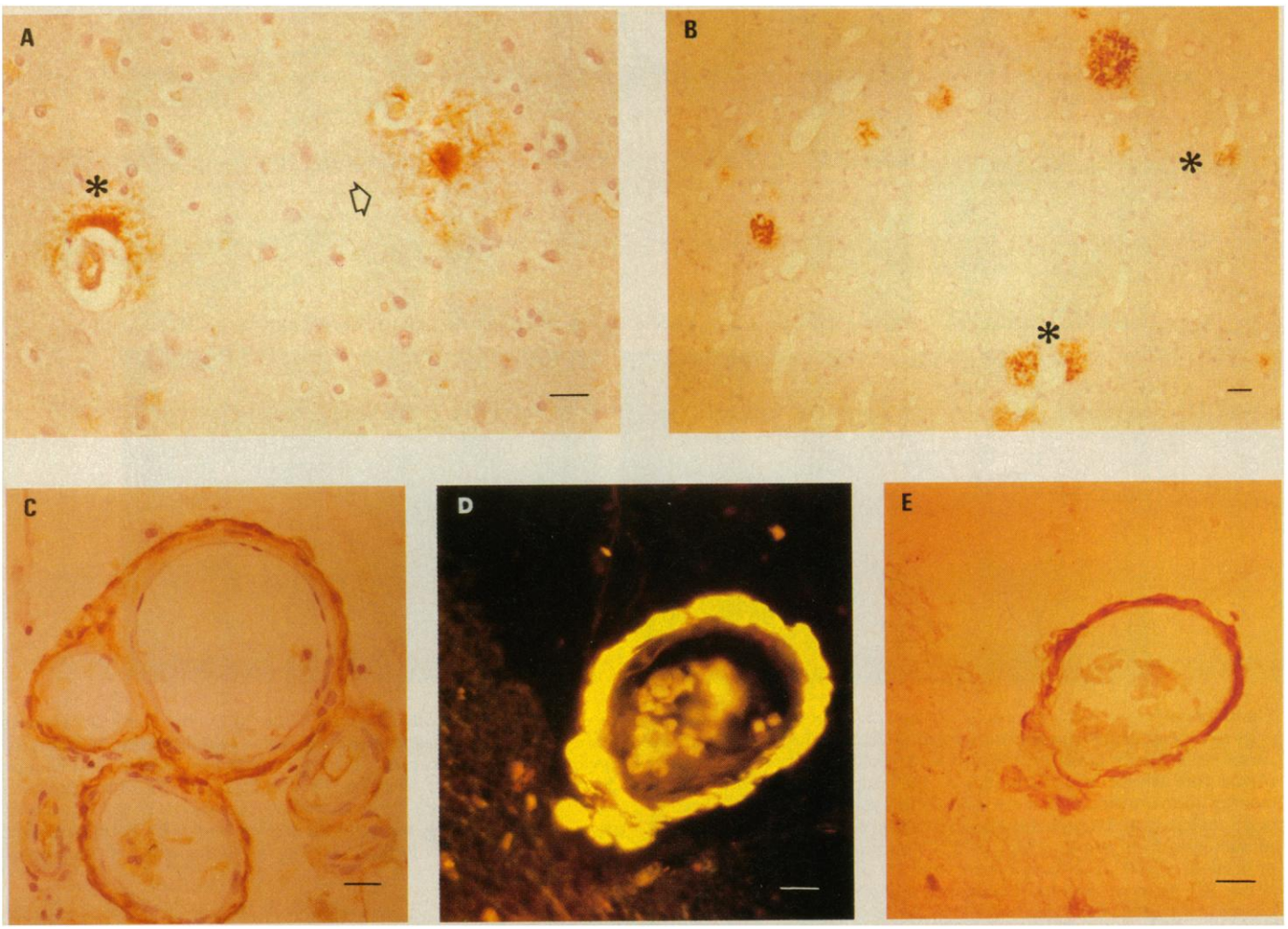

Fig. 1. Immunocytochemistry of amyloid deposits in aged mammalian brain with antibodies (1:250) to amyloid proteins from human (AD) brain (avidin-biotin-peroxidase technique). (**A**) Human cerebral cortex from a patient with AD reacted with antiserum A shows typical amyloid deposits in a neuritic plaque (arrow) and a cortical vessel (*). (**B**) Multiple amyloid plaques in rhesus monkey cortex labeled with antiserum A, including some perivascular plaques (*). (**C**) Human (AD) meningeal blood vessels stained with antiserum S display extensive amyloid deposits. (**D** and **E**) Comparison of thioflavin staining (D) and antiserum S (E) on a double-labeled meningeal vessel in the cerebral cortex of a 46-year-old orangutan. Note the precise overlap of thioflavin fluorescence and immunoperoxidase reaction. Bars, 20 μm.

from AD brain (*5*) abolished the labeling of amyloid plaques and vessels in primate brain (Fig. 2B) and polar bear brain, and markedly reduced or abolished the staining of these lesions in human brain. Absorption of antiserum C (previously shown by enzyme-linked immunosorbent assay to have high-titer activity against the synthetic AD amyloid peptide) and antiserum B with the synthetic peptide abolished their staining of both animal (Fig. 2C) and human amyloid deposits. In view of the mixed nature of antisera S and V (that is, both amyloid- and PHF-reactive), we absorbed them with brain microtubule–associated protein fractions markedly enriched in tau. This absorption markedly decreased the staining of NFTs and plaque neurites in human brain sections, but did not significantly alter the staining of plaque and vascular amyloid in monkey and human brains.

Thus, we found a highly similar pattern of antigenic reactivities for the cerebral and cerebrovascular amyloid filaments that accumulate with aging in three species of nonhuman primates, the dog, the polar bear, and humans with AD. All five polyclonal antibodies against AD brain amyloid proteins cross-reacted with the amyloid deposits in animal brains, and absorption with human amyloid filaments abolished amyloid reactivity in both humans and animals. Moreover, an antibody to a 28-residue peptide that is the only AD amyloid protein sequence currently reported reacted with the amyloid deposited in blood vessels and cortical plaques of nonhuman primates and other mammals during aging. The relative intensity of amyloid staining among the five antisera, a reflection of the number and surface exposure of their respective antigens in the amyloid filaments, was virtually identical in humans and animals. Antibodies raised against intact human amyloid filaments (S and V), to a low molecular weight protein extracted from these filaments (A and C), and to a synthetic peptide having the NH_2-terminal sequence of a human amyloid protein (B) all showed similar reactions with brain amyloid of human, rhesus monkey, squirrel monkey, orangutan, polar bear, and dog.

Previous studies have described the microscopic features of senile plaques in aged rhesus monkeys (*8*) and dogs (*9*) and the neurotransmitter specificities of some of the altered neurites in monkey plaques (*10–12*). This report provides information about the antigenic composition of brain amyloid in species other than humans. Although the amyloid filaments in aged animals appear structurally and immunochemically indistinguishable from human brain amyloid filaments, the dystrophic neurites that surround the amyloid plaques in lower mammals have not been found to contain PHFs (*8, 9*). This morphological difference is confirmed by our immunochemical results: the neurites of monkey plaques were not labeled by a PHF antiserum (P) or by tau antibodies (DJ),

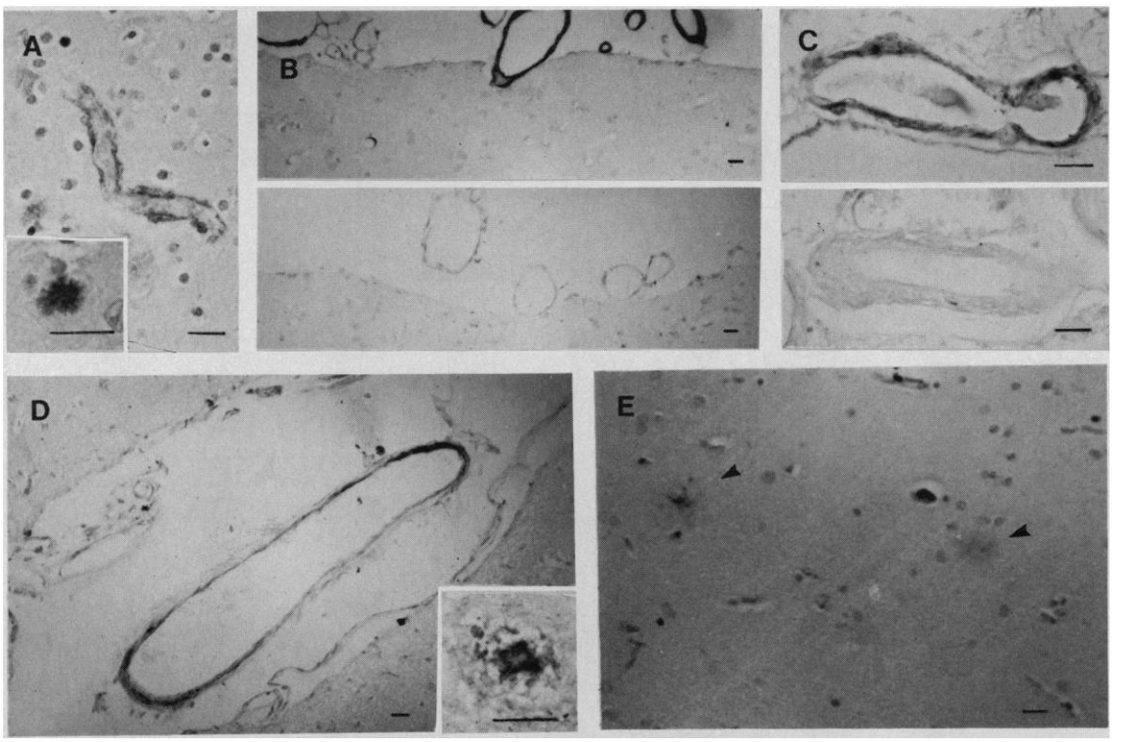

Fig. 2. Immunocytochemistry of amyloid deposits in aged mammalian brain with antibodies (1:250) to amyloid proteins. (**A**) Squirrel monkey cerebral cortex stained with antiserum S reveals an amyloidotic microvessel. Inset, a plaque core labeled with antiserum A. (**B**) Adjacent sections of rhesus monkey cortex reacted with antiserum A show staining of amyloid-bearing vessels before (top) but not after (bottom) absorption with purified amyloid plaque cores from human (AD) brain. Absorption was accomplished by incubation of 100 μg of core protein with 20 μl of serum at 4°C for 16 hours. (**C**) Adjacent sections of orangutan cortex reacted with antiserum C show labeling of vascular amyloid before (top) but not after (bottom) absorption with a 28–amino acid synthetic peptide from a human (AD) amyloid protein. Absorption was accomplished by incubating 150 μg of peptide with 20 μl of serum at 4°C for 16 hours. (**D**) Amyloid-bearing meningeal vessel is labeled with antiserum A in an aged dog. Inset, amyloid plaque in another dog reacted with antiserum A. (**E**) Polar bear cortex reacted with antiserum A shows labeling of two amyloid plaques (arrowheads). Bars, 20 μm.

both of which strongly stain the PHF-containing neurites of human senile plaques (*13–15*). The neurofilament antibody RT97, which labels NFTs and plaque neurites in AD brain (*17*), also identified the neurites of senile plaques in the aged monkey. These results suggest that neurofilament proteins, but not tau proteins, are present in the altered neurites of senile plaques in nonhuman mammals and that tau is associated with the PHF structure.

The animal brains examined here also failed to show PHF reactivity in neuronal cell bodies (that is, NFTs), in agreement with prior studies. The lack of NFTs but presence of amyloid in these aged animals argues against the notion that the amyloid proteins in plaque cores and blood vessels in AD originate from intraneuronal PHF proteins (*18*). In humans, NFTs occur in a variety of etiologically unrelated neurological disorders, whereas amyloid-containing neuritic plaques are generally restricted to three conditions—normal aging, AD, and the AD-type degeneration that occurs late in Down syndrome. PHFs, which seem to represent insoluble aggregates of altered neuronal cytoskeletal proteins including tau, may occur as a relatively nonspecific response of human neurons to various insults, but apparently do not form in the neurons of nonhuman primates. In contrast, the development of cortical foci of dystrophic neurites, often if not always (*6*) associated with amyloid in the center of these foci and in adjacent microvessels, is an age-related process that is shared by several mammalian species, including humans. Because this process is seen in normal aged humans and primates, its more severe, widespread expression in AD brain may represent an acceleration or "escape from control" of a normal involutional process in the aged mammalian nervous system. Such a model may be particularly valid in genetic (autosomal dominant) forms of AD and in Down syndrome. Our data have implications for theories about the pathogenesis of AD. They indicate that the amyloid filaments in aged mammals arise from proteins closely related to those in humans with AD and Down syndrome, although AD could possibly involve specific mutations of an amyloid subunit protein that accumulates in normal brain aging.

Despite the absence of PHFs and NFTs, the aged nonhuman primate is a biochemically relevant model for certain important features of AD. Ultrastructural, biochemical, and molecular biological studies of in situ and cultured vascular and glial cells from monkeys or dogs during aging may provide information about the mechanisms of cerebrovascular amyloidosis and neuritic plaque formation not obtainable from studies of postmortem human brain.

REFERENCES AND NOTES

1. B. E. Tomlinson and J. A. N. Corsellis, in *Greenfield's Neuropathology*, J. H. Adams, J. A. N. Corsellis, L. W. Duchon, Eds. (Arnold, London, 1984), pp. 951–1025.
2. G. G. Glenner, J. H. Henry, S. Fujihara, *Ann. Pathol.* **1**, 120 (1981); C. T. Vanley, M. J. Aguilar, R. J. Kleinhenz, M. D. Lagios, *Hum. Pathol.* **12**, 609 (1981); G. G. Glenner, in *Biological Aspects of Alzheimer's Disease*, R. Katzman, Ed. (Cold Spring Harbor Laboratory, Cold Spring Harbor, NY, 1983), pp. 127–144; C. L. Joachim, J. Morris, D. J. Selkoe, *Neurology* **36** (suppl. 1), 226 (1986).
3. C. W. Wong, V. Quaranta, G. G. Glenner, *Proc. Natl. Acad. Sci. U.S.A.* **82**, 8729 (1985).
4. C. L. Masters *et al.*, *ibid.*, p. 4245.
5. D. J. Selkoe, C. R. Abraham, M. B. Podlisny, L. K. Duffy, *J. Neurochem.* **46**, 1820 (1986).
6. T. Miyakawa, A. Shimoji, R. Kuramoto, Y. Higuchi, *Virchows Arch. B* **40**, 121 (1982).
7. B. E. Tomlinson, G. Blessed, M. Roth, *J. Neurol. Sci.* **7**, 331 (1968).
8. H. M. Wisniewski, B. Ghetti, R. D. Terry, *J. Neuropathol. Exp. Neurol.* **32**, 566 (1973).
9. H. M. Wisniewski, A. B. Johnson, C. S. Raine, W. J. Kay, R. D. Terry, *Lab. Invest.* **23**, 287 (1970).
10. R. G. Struble, L. C. Cork, P. J. Whitehouse, D. L. Price, *Science* **216**, 413 (1982).
11. R. G. Struble, D. L. Price, Jr., L. C. Cork, D. L. Price, *Brain Res.* **361**, 267 (1985).
12. C. A. Kitt *et al.*, *Science* **226**, 1443 (1984); L. C. Walker *et al.*, *Neurosci. Lett.* **59**, 165 (1985); R. G.

Struble, C. A. Kitt, L. C. Walker, L. C. Cork, D. L. Price, *Brain Res.* **324**, 394 (1984); C. A. Kitt *et al.*, *Neuroscience* **16**, 691 (1985).
13. Y. Ihara, C. Abraham, D. J. Selkoe, *Nature (London)* **304**, 727 (1983).
14. K. S. Kosik, C. L. Joachim, D. J. Selkoe, *Proc. Natl. Acad. Sci. U.S.A.* **83**, 4044 (1986).
15. N. Nukina and Y. Ihara, *J. Biochem.* **99**, 1541 (1986); I. Grundke-Iqbal *et al.*, *J. Biol. Chem.* **261**, 6084 (1986); J. G. Wood, S. S. Mirra, N. J. Pollock, L. I. Binder, *Proc. Natl. Acad. Sci. U.S.A.* **83**, 4040 (1986); Y. Ihara, N. Nukina, R. Miura, M. Ogawarra, *J. Biochem.* **99**, 1807 (1986); I. Grundke-Iqbal *et al.*, *Proc. Natl. Acad. Sci. U.S.A.* **83**, 4913 (1986).
16. G. G. Glenner and C. W. Wong, *Biochem. Biophys. Res. Commun.* **120**, 885 (1984).
17. B. H. Anderton *et al.*, *Nature (London)* **298**, 84 (1982).
18. C. L. Masters *et al.*, *EMBO J.* **4**, 2757 (1985).
19. We thank L. Galibert and J. Morris for technical assistance in some aspects of this project; B. Anderton for providing monoclonal antibody RT97; K. Kosik for providing antiserum DJ; and B. Hansen, K. Keenan, and R. Snyder for providing certain tissues. Supported in part by PHS grants AG06173 (D.J.S.), NS23340 (D.J.S.), AG05134 (Massachusetts Alzheimer's Disease Research Center), NS20471 (D.L.P.), AG05146 (D.L.P.), DK37737, and RR00130, and gifts from the Robert L. and Clara G. Patterson Trust and the Claster family.

8 October 1986; accepted 16 January 1987

Characterization and Chromosomal Localization of a cDNA Encoding Brain Amyloid of Alzheimer's Disease

DMITRY GOLDGABER, MICHAEL I. LERMAN, O. WESLEY MCBRIDE, UMBERTO SAFFIOTTI, D. CARLETON GAJDUSEK

Four clones were isolated from an adult human brain complementary DNA library with an oligonucleotide probe corresponding to the first 20 amino acids of the β peptide of brain amyloid from Alzheimer's disease. The open reading frame of the sequenced clone coded for 97 amino acids, including the known amino acid sequence of this polypeptide. The 3.5-kilobase messenger RNA was detected in mammalian brains and human thymus. The gene is highly conserved in evolution and has been mapped to human chromosome 21.

WE REPORT THE ISOLATION AND characterization of complementary DNA (cDNA) clones coding for the polypeptide that forms the brain amyloid of paired helical filaments of neurofibrillary tangles within neurons, the extracellular amyloid plaque cores, and the vascular wall amyloid deposits in Alzheimer's disease (AD) and adult Down syndrome (DS) (*1–3*). This is the same amyloid in the paired helical filaments in neurofibrillary tangles of Guamanian amyotrophic lateral sclerosis parkinsonism dementia and of the amyloid in the aging brain (*4*).

Computer analysis of the 28–amino acid sequence of the polypeptide (*1–3*) revealed that the first 20 amino acids included unique regions not found in known sequences deposited in computer banks of protein sequences. A 59-residue oligonucleotide probe corresponding to these first 20 amino acids was synthesized with deoxyinosine in every third position (Fig. 1) (*5–7*).

Four clones (λAm1, λAm2, λAm3, and λAm4) were isolated from a λgt11 cDNA library derived from human brain (*8, 9*) by screening with this synthesized oligonucleotide probe. Restriction maps of the four positive cDNA clones revealed that they were identical, except for λAm1, which was approximately 100 bp longer than the other three and contained an internal Eco RI site (Fig. 2).

```
   asp ala glu phe arg his asp ser gly tyr
5'-GAI GCI GAI TTI AGI CAI GAI TCI GGI TAI
                  C       AG  T

   glu val his his gln lys leu val phe phe
   GAI GTI CAI CAI CAI AAI CTI GTI TTI T[T]-3'
                       T

   ala glu asp val gly ser asn lys
```

Fig. 1. The 59-base oligonucleotide probe with the deoxyinosine (I) in every third position (first line), corresponding to the first 20 amino acids of the published 28–amino acid sequence (second line) for brain amyloid of Alzheimer's disease and adult Down syndrome (*2*).

Southern blot analysis of the λAm4 clone showed that the 59–amino acid probe hybridized to the Eco RI–Pvu II fragment at the 5′ end of the insert. The whole 1-kb Eco RI insert of clone λAm4 was subcloned in the plasmid pGEM-3 and its fragments were cloned in the plasmid pGEM blue (*10*) and sequenced by the chain termination method (Fig. 2) (*11*). The sequence contained an open reading frame, which has been translated into an amino acid sequence.

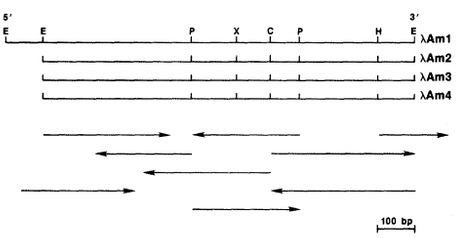

Fig. 2. Restriction maps of the four cDNA clones λAm1 through λAm4 isolated from adult human brain λgt11 cDNA library and the sequencing strategy of the λAm4 clone. The λAm2, λAm3, and λAm4 clones were about 1 kb; λAm1 was about 100 bp longer and contained an internal Eco RI site. Restriction enzyme sites: E, Eco RI; P, Pvu II; C, Cla I; X, Xmn I; and H, Hind III. The arrows represent pGEM blue subclones, direction of sequencing, and length of sequence derived by the chain termination ("dideoxy") method (*11*) with the use of unique restriction sites for subcloning and the sequencing protocol from Promega Biotec (*10*).

The deduced 97–amino acid sequence from the first 291 nucleotides included the sequence for amino acids 3 to 42 of the brain amyloid polypeptide of AD and DS (*1–3, 12, 13*). Beyond amino acid 42, which is the termination of the brain amyloid polypeptide from AD and DS patients, there are another 57 amino acids and a TAG termination codon (Fig. 3). The nucleotide sequence of the cDNA clone and the deduced amino acid sequences had no extensive homology to any previously known sequences (*14*).

Hydropathy analysis (*15*) of the deduced amino acid sequence showed a large hydrophobic domain and alternating hydrophobic and hydrophilic regions typical for membrane proteins (Fig. 4). This structure could possibly result in aggregate formation. Secondary structure predictions were made with the methods of Chou and Fasman and Garnier *et al.* (*16, 17*). There was a strong tendency for the polypeptide to form a β-pleated sheet configuration in amino acids 31 to 50 (Fig. 4A), which is consistent with the known structure of amyloid (*18, 19*). In conversion of the precursor protein to amyloid, cleavage should occur between amino acid 42 and amino acid 43, which lie within the main hydrophobic domain. There are two potential *N*-glycosylation sites (Asn-X-Thr/Ser) at positions 84 and 88. It is unknown whether this protein is glycosylated, but amino acid 88 is unlikely to be glycosylated because it has an adjacent proline residue (Fig. 3) (*20, 21*). A fusion protein of 126 kD was produced in *Escherichia coli* Y1089. The size of the recombinant part of this protein (12 kD) is consistent with the estimated size of the deduced polypeptide.

Northern blot analysis of polyadenylated RNA (*9*) was performed with the 1-kb Eco RI fragment of the λAm4 clone (the Am4 probe) under high stringency conditions. A single band of about 3.5 kb was detected in

D. Goldgaber and D. C. Gajdusek, Laboratory of Central Nervous System Studies, National Institute of Neurological and Communicative Disorders and Stroke, National Institutes of Health, Bethesda, MD 20892.
M. I. Lerman and U. Saffiotti, Laboratory of Experimental Pathology, National Cancer Institute, National Institutes of Health, Bethesda, MD 20892.
O. W. McBride, Laboratory of Biochemistry, National Cancer Institute, National Institutes of Health, Bethesda, MD 20892.